EPJ Web of Conferences **37**, 05009 (2012)
DOI: 10.1051/epjconf/20123705009

Measurement of $\gamma\gamma^* \to \pi^0$ transition form factor at Belle

Sadaharu Uehara[a] for the Belle Collaboration

KEK, Institute of Particle and Nuclear Studies, High Energy Accelerator Research Organization, Tsukuba, Japan

Abstract. We report a measurement of the process $\gamma\gamma^* \to \pi^0$ with a 759 fb^{-1} data sample recorded with the Belle detector at the KEKB asymmetric-energy e^+e^- collider. The pion transition form factor, $F(Q^2)$, is measured for the kinematical region 4 GeV$^2 \lesssim Q^2 \lesssim$ 40 GeV^2, where $-Q^2$ is the invariant mass squared of a virtual photon. The measured values of $Q^2|F(Q^2)|$ agree well with the previous measurements below $Q^2 \simeq 9$ GeV^2 but do not exhibit the rapid growth in the higher Q^2 region seen in another recent measurement, which exceeds the asymptotic QCD expectation by as much as 50%.

1 Introduction

A measurement of the transition form factor of two photons to a pion provides opportunity of a useful test for QCD. It is measured and calculated based on the diagram shown in Fig. 1. One photon is highly virtual, and the virtuality of the photon (Q^2) is expressed by the squared mass with an inverted sign. The other photon is almost real, and its finite-Q^2 effect in the measurement is corrected to match the real photon.

Theoretically, the transition form factor $F(Q^2)$ is calculated with a distribution amplitude of quarks inside a pion and is factorized with the hard scattering amplitude for quarks, as well as the pion decay constant. At the high Q^2 limit, it provides a definite prediction of the asymptotic value.

The form factor is experimentally derived from a measurement of the differential cross section, $d\sigma/dQ^2$, applying a conversion factor which is calculated based on QED, for the process $e^+e^- \to (e)e\pi^0$, where e and (e) in the final state are a tagged and an untagged electron, respectively. The normalization of the conversion is connected to the two-photon decay width of the pion.

The BaBar collaboration has reported a measurement of the π^0 transition form factor in 2009 [1]. Their measurement covers the Q^2 region above 10 GeV^2 for the first time, and there, the form factor goes above the prediction of the asymptotic QCD value with a rather steep increase. It seems to exceed it by as much as 50% in the highest Q^2 region in the measurement. This result has attracted interests of many theoretical physicists [2]. An independent measurement of the pion form factor is thus very important, and we have performed a verification using Belle data [3].

2 Measurement and data reduction

We detect signal events consisting of a recoil electron (or positron) at the tag side and the two photons from a π^0 decay. As the KEKB accelerator and Belle detector are asymmetric with respect to the electron and positron beams, kinematical coverage is different between the two tag sides [4]. We measure the differential cross section with a positron-tag (p-tag) and an electron-tag(e-tag), separately, for a consistency check before combining them.

[a] e-mail: uehara@post.kek.jp

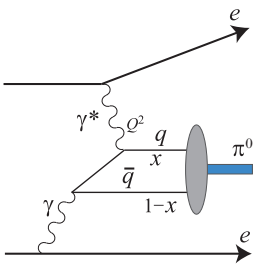

Fig. 1. A Feynman diagram for $\gamma\gamma^* \to q\bar{q} \to \pi^0$ in e^+e^- collisions

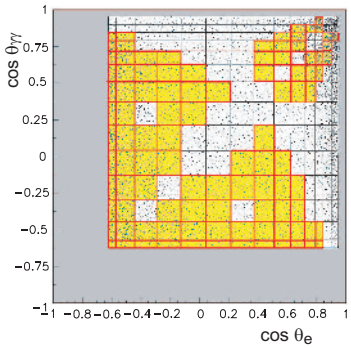

Fig. 2. Two-dimensional angular regions in ($\cos\theta_e$, $\cos\theta_{\gamma\gamma}$) defined as the Bhabha mask. Events in the hatched regions with complicated shape are selected.

Event triggers to collect the signals events are provided by the electromagnetic calorimeter system (ECL). The main trigger logic, the HiE trigger (total energy trigger with a high-energy threshold), is vetoed by the Bhabha trigger logic (the CsiBB trigger) that detects Bhabha events in order not to record them because of its enormously high rate (Bhabha veto). This mechanism brings a significant loss of the efficiency for the present signal process as a side effect with reducing a fraction of the acceptance. This condition is in contrast to the BaBar measurement where a special salvaging mechanism for this type of events has been prepared.

We have used data corresponding to an integrated luminosity of 759 fb^{-1}. In selection of the signal-candidate events, we require just one track loosely identified as an electron and two photons from a π^0 decay. In order to cope with a large background from radiative Bhabha process, we require energy symmetry for the two photons as well as a large enough polar-angle difference between them; the latter condition is to reject photon conversions to an electron-pair which fake two photons in the calorimeter, using that the conversion trajectories tend to lie on a plane perpendicular to the magnetic field of the spectrometer.

In addition, we impose a complicated selection condition for the polar angles of the electron and the two-photon system which we call Bhabha mask (Fig. 2), in order to reduce an uncertainty of the trigger inefficiency caused by the Bhabha veto. Only the specified two-dimensional angular regions in the figure are used as an acceptance for the signal events; the inefficiency due to the veto is serious in the other regions.

Figure 3 shows the event distribution in a middle of signal selection referring to the energy of the detected two photons. Three-body kinematics for the process $e^+e^- \to (e)e\pi^0$, $\pi^0 \to \gamma\gamma$ constrains the energy of the two-photon system when the measured values of electron momentum and the two-photon direction are provided. The ratio between the measured and expected energies, $E_{\rm ratio}$, is used to separate signal candidates from π^0 backgrounds.

3 Calibration of the Bhabha trigger

We have used radiative Bhabha events with a configuration called virtual Compton (VC) scattering ($e^+e^- \to (e)e\gamma$) for a calibration of the CsiBB trigger. The event topology resembles to that of the signal process. We define Q^2 for the detected electron in this process in the same way as for the signal process.

Combining event samples collected by the HiE trigger and by the CsiBB trigger (the latter taken with a prescale factor 50) and compensating the effect from the Bhabha veto statistically, we determine the trigger efficiency as a function of the energy deposit. We have used Monte Carlo (MC) events generated by Rabhat program [5] for the scattering process and fed to the trigger simulator code. We thus tuned the thresholds of the CsiBB trigger to match the experimental determinations of the efficiency.

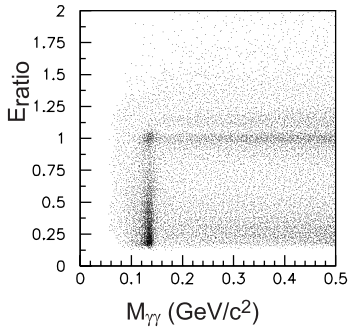

Fig. 3. Scatter plots for $E_{\rm ratio}$ vs. $\gamma\gamma$ invariant mass for experimental data.

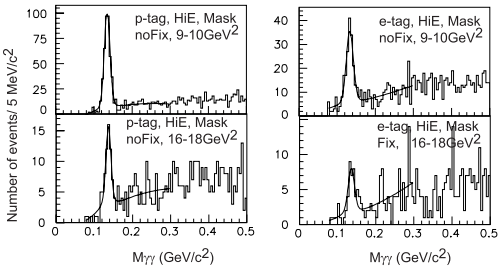

Fig. 4. Results of the fit to the experimental $M_{\gamma\gamma}$ distributions for some selected Q^2 bins.

The Rabhat MC provides a QED calculation of the cross section for the radiative Bhabha process in the VC configuration, and we compare the experimental yield to the MC after the tuning of the trigger simulation in various distributions to confirm a validity of the efficiency determination. We also compare the Bhabha-mask and -veto efficiencies between the trigger simulator and the data. This study validates our trigger efficiency within a 10% level.

Finally, we obtain Q^2 dependence of the efficiency for the signal process, using the signal MC, for p-tag and e-tag, separately.

4 Derivation of differential cross section

We extract π^0 signal yields with a fit to the two-photon invariant mass distribution in different Q^2 bins, as shown in Fig. 4 for some selected Q^2 bins, where we employ double Gaussian function for the signal peak, for which the shape parameters are partially determined by the MC and the second-order polynomial function for the background component. The background contribution comes mainly from a higher-order QED $(e)e\gamma\gamma$ process.

The Q^2 dependence is unfolded using an inverted migration matrix which is determined by MC to compensate inter-bin migration due to initial-state radiation from the tagged side electron and the finite resolution effect in measurement of the electron momentum.

We subtract peaking backgrounds from the signal candidate yields, studying some background processes that produce pions. We find the backgrounds from e^+e^- annihilation events, including those with a tagged electron from particle misidentification, are negligibly small from a study of wrong-sign events for the electron charge in relation to the longitudinal momentum of the detected system along the beam axis.

We find background contributions from $(e)e\pi^0\pi^0$ and $(e)e\pi^0\gamma$ production processes; the former is a single-tag two-photon process and the latter is production of a ρ^0 or ω meson decaying to $\pi^0\gamma$. We actively collect and measure the yield of these processes with requiring an additional pion or a photon to study the background size. The observed yields are put into a specially produced MC generator for the background processes, and contaminations in the signal sample are estimated. The results are about 2% (0.8% – 3%, depending on a Q^2 bin) from the $\pi^0\pi^0$ ($\pi^0\gamma$) process. These contributions are subtracted from the measured signal yield.

The differential cross sections are obtained for p-tag and e-tag separately. As the measurements from the two tags are consistent with each other, we combine them (Fig. 5).

Among systematic uncertainties from different sources which are assigned to the cross section, the biggest contributions come from the extraction of the π^0 yield with a fit and the uncertainty of the trigger efficiency; they largely depend on the Q^2 regions. The total systematic error for the combined cross section is between 8% and 14%, depending on the Q^2 region.

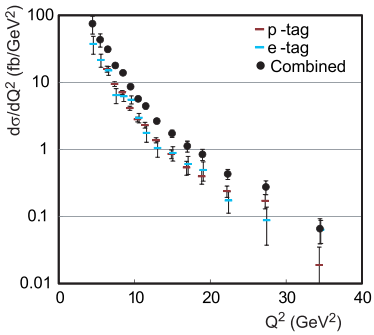

Fig. 5. Results for the $e^+e^- \to (e)e\pi^0$ differential cross section. "Combined" corresponds to twice the weighted average of the p-tag and e-tag results. Error bars show statistical uncertainties only.

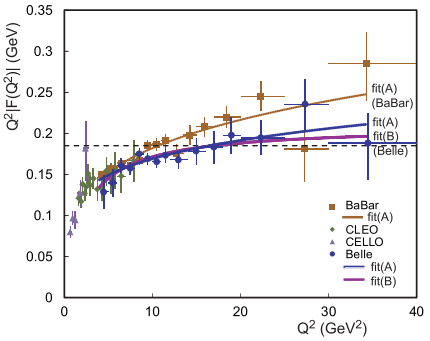

Fig. 6. Comparison of the results for the product $Q^2|F(Q^2)|$ for the π^0 from different experiments. The curves are from the fits (A) and (B), and the dashed line shows the asymptotic prediction from pQCD (~ 0.185 GeV).

5 π^0 transition form factor

The differential cross section is translated to the transition form factor multiplied by the Q^2, $Q^2|F(Q^2)|$, using the calculated conversion factor.

We show the Belle result for the transition form factor in Fig. 6, as well as the results of the previous measurements. It is compared with the asymptotic QCD prediction shown by the dashed line. Our result is close to the line at the highest Q^2 region. The Q^2 dependence of the Belle data is smoother than the BaBar results and does not show a rapid growth above 10 GeV^2.

We try a parameter fit for the Q^2 dependence of the form factor with the function suggested by BaBar, $\sim (Q^2/10\ \text{GeV}^2)^\beta$ (fit(A)). Each of our fit results for the size and slope parameters differs from the corresponding BaBar's value by about 1.5σ to the smaller side. We also try a fit to another parameterization with an asymptotic limit, $\sim Q^2/(Q^2+C)$ (fit(B)). The obtained fit for the asymptotic value, 0.209 ± 0.016 GeV, is slightly larger than the QCD prediction but still consistent with it. The fit curves are also shown in Fig. 6.

6 Summary

We have measured the neutral pion transition form factor for the process $\gamma\gamma^* \to \pi^0$ in the region $4\ \text{GeV}^2 \lesssim Q^2 \lesssim 40\ \text{GeV}^2$ with a 759 fb^{-1} data sample collected with the Belle detector at the KEKB asymmetric-energy e^+e^- collider. The measured values of $Q^2|F(Q^2)|$ agree with the previous measurements [6,7,1] for $Q^2 \lesssim 9\ \text{GeV}^2$. In the higher Q^2 region, in contrast to BaBar, our results do not show a rapid growth with Q^2, and they are closer to theoretical expectations.

References

1. B. Aubert *et al.* (BaBar Collaboration), Phys. Rev. D **80**, 052002 (2009).
2. S.J. Brodsky, F.-G. Cao and G.F. de Téramond, Phys. Rev. D **84**, 033001 (2011); Phys. Rev. D **84**, 075012 (2011); most of earlier theoretical attempts are listed in these articles.
3. S. Uehara, Y. Watanabe, H. Nakazawa *et al.* (Belle Collaboration), arXiv:1205.3249[hep-ex] (2012), submitted to Phys. Rev. D, and references therein.
4. A. Abashian *et al.* (Belle Collaboration), Nucl. Instr. and Meth. A **479**, 117 (2002).
5. K. Tobimatsu and Y. Shimizu, Comp. Phys. Comm. **55**, 337 (1989).
6. H.J. Behrend *et al.* (CELLO Collaboration), Z. Phys. C. **49**, 401 (1991).
7. J. Gronberg *et al.* (CLEO Collaboration), Phys. Rev. D **57**, 33 (1998).